Discrepancies Between Saclay and Livermore Photoneutron Cross Sections

E. WOLYNEC and M.N. MARTINS

Instituto de Física, Universidade de São Paulo, Caixa Postal 20516, São Paulo, 01498, SP, Brasil

Abstract The differences between the Saclay and Livermore photoneutron cross sections are discussed. It is shown that the differences between their (γ,n) and $(\gamma,2n)$ cross sections arise from the neutron multiplicity sorting. Measurements of the (e,n) and $(e,2n)$ cross sections in ^{181}Ta show that Livermore has the correct multiplicity sorting. The implications of these results are discussed.

1. INTRODUCTION

The giant dipole resonance has always been of central interest in photonuclear reaction studies, both theoretical and experimental. It corresponds to the fundamental frequency for absorption of electric dipole radiation by the nucleus as a whsle.

Over the past three decades many studies of photonuclear reactions have been made, for many nuclei through the periodic table, in the attempt to delineate the systematics of photon absorption by nuclei in general and of the giant electric dipole resonance, which dominates the absorption process at energies between 10 and 30 MeV, in particular. The large effort that has been put into these studies is justified by the fact that the theory of the interaction of eletromagnetic radiation with nuclei is perhaps the best understood in nuclear physics: if the interaction in the entrance channel is understood, then the effects o'f the purely nuclear forces can be studied directly by rneasuring either the photon absorption cross sections or the products of nuclear photo-disintegration.

Most of the work in this area was carried out at two laboratories, Saclay and Livermore, measuring photoneutron cross sections using monoenergetic photon beams. The combined studies of these two laboratories span the whole periodic table, in a quite complete systematics of the El giant resonance. The use of monoenergetic photon beams has given rise to cross section measurements with high resolution, and es-

pecially to an improved knowledge of the cross sections above the peak of the giant resonance. Higher-multiplicity cross sections have beer measured directly and their systematics studied, and more accurate information on structure throughout the giant resonance obtained. The qual. ity of the data produced has justified well the effort necessary to develop and utilize monoenergetic photon beams.

From those detailed studies many important properties of the E1 giant resonance have been obtained. There is, however, a serious conflict between the data from those Laboratories. There are systematic differences in the shapes and magnitudes of their (γ,n) and $(\gamma,2n)$ cross sections. Because of these differences, from the Saclay data it turns out that for heavy nuclei there is 15-20% of direct contribution in the reaction rnechanism, while the Livermore data support a dominant statitiscal decay of the E1 giant resonance.

The majority of the results available are compi1ed in the *Atlas of Photoneutron Cross Sections obtained with Monoenergetic Photons*[1]. There are also a few review articles on the subject[1,2] but none of these publications has addressed the problem of the differences between the measurements performed at Saclay and Livermore. In this paper we compare the Saclay and Livermore measurements for the nuclei listed in table 1. We show, as already mentioned in a comment[15], that both laboratories measure the same number of neutrons versus the photon incident energy but arrive at different partial cross sections as a consequence of the analysis that separates the observed neutrons into (γ,n) and $(\gamma,2n)$ events. Experimental results of the (e,n) and $(e, 2n)$ cross sections of ^{181}Ta obtained at our laboratory indicate that Livermore is the laboratory that performs correctly the neutron multiplicity sorting.

The typical differences between Saclay and Livermore data are illustrated in fig. 1, where the (γ,n) measurements from Saclay and Livermore are shown. The results from Livermore are multiplied by 1.06 in order to show both cross sections in the same absolute scale. The cross sections are in good agreement up to the $(\gamma,2n)$ threshold, Above this energy there is an important difference: the Livermore cross section vanishes a few MeV above the $(\gamma,2n)$ threshold, in good agreement with the predictions of the statistical model, while the Saclay cross

Table I - Nuclei measured at Saclay (S) and Livermore (L).

| Nucleus	$\int \sigma_{\gamma,n}(E_\gamma)dE_\gamma$ a) (MeV.mb)	$\int \sigma_{\gamma,2n}(E_\gamma)dE_\gamma$ a) (MeV.mb)	Ref.	R
[89]Y	1279 S 960 L	74 S 99 L	3 4	1.255 ± 0.005
[115]I	1470 S 1354 L	278 S 508 L	5 6	0.942 ± 0.004
[117]Sn	1334 S 1380 L	220 S 476 L	5 6	1.012 ± 0.007
[118]Sn	1377 S 1302 L	258 S 531 L	5 6	1.056 ± 0.005
[120]Sn	1371 S 1389 L	399 S 673 L	5 6	0.987 ± 0.004
[124]Sn	1056 S 1285 L	502 S 670 L	5 6	0.929 ± 0.006
[133]Cs	1828 S 1475 L	328 S 503 L	5 7	1.106 ± 0.007
[159]Tb	1936 S 1413 L	605 S 887 L	8 9	1.062 ± 0.0011
[165]Ho	2090 S 1735 L	766 S 744 L	8 10	1.136 ± 0.007
[181]Ta	2180 S 1300 L	790 S 881 L	8 11	1.218 ± 0.018
[197]Au	2588 S 2190 L	479 S 777 L	12 13	1.004 ± 0.013
[208]Pb	2731 S 1776 L	328 S 860 L	12 14	1.296 ± 0.011
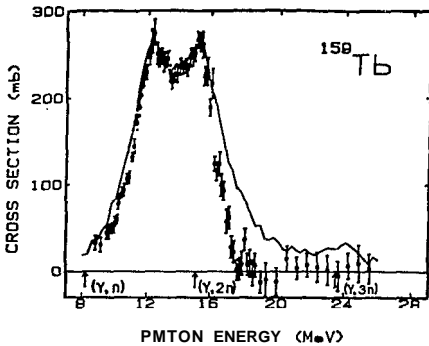
Fig.1 - (γ,n) cross sections from Saclay (solid line) and Livermore (experimental points) for ^{159}Tb. The Livermore data are multiplied by 1.06 in order to show both measurements at the same absolute scale.

section exhibits a tail. In'ref. 8, the observed tail of the Saclay cross section is interpreted as arising from fast neutrons that would have escaped detection in the Livermore measurement, leading to the conclusion that for ^{159}Tb the contribution of the *direct effect* in'the photoneutron cross section is $n_d = 23 \pm 4$ percent. In table 2 the percentages of direct neutrons inferred at Saclay are given for several nuclei.

Figure 2 shows the $(\gamma,2n)$ cross sections from Saclay and Livermore. The $(\gamma,2n)$ cross sections differ in shape and magnitude, the Livermore one being much bigger. Even though up to the $(\gamma,2n)$ threshold the (γ,n) cross sections from Livermore, $\sigma_{\gamma,n}^{L}$, and Saclay, $a_{\gamma,n}^{S}$, differ by only 6 percent in the absolute scale, their integrated cross sections up to 28 MeV are 1413 and 1936 MeV.mb, respectively. While the integrated (γ,n) cross section from Saclay is 37% bigger than the Livermore result, their integrated $(\gamma,2n)$ cross section is 47% smaller.

2. ANALYSIS OF THE PHOTONEUTRON DATA

In order to understand these differences we reconstructed the total neutron measurements from Saclay and Livermore

$$\sigma_{\gamma,Tn} = \sigma_{\gamma,n} + 2\sigma_{\gamma,2n} + 3\sigma_{\gamma,3n} \tag{1}$$

using their published $\sigma_{\gamma,n}$, $\sigma_{\gamma,2n}$ and $\sigma_{\gamma,3n}$ cross sections, which are available in digital form . It is interesting to compare $\sigma_{\gamma,Tn}$ from both

Table 2 - Percentage of direct neutrons obtained at Saclay.

Nucleus	n_d (%)	References
^{94}Mo	25 ± 7	16
^{96}Mo	15 ± 7	16
^{98}Mo	10 ± 7	16
^{100}Mo	11 ± 7	16
^{139}La	28 ± 5	8
^{140}Ce	12 ± 3	17
^{142}Ce	10 ± 3	17
^{Nat}Sm	10 ± 3	17
^{159}Tb	23 ± 4	8
^{165}Ho	23 ± 4	8
^{Nat}Er	11 ± 3	17
^{175}Lu	15 ± 3	17
^{181}Ta	22 ± 2	8
^{197}Au	20 ± 4	12
^{208}Pb	15 ± 4	12
^{238}U	14 ± 2	18
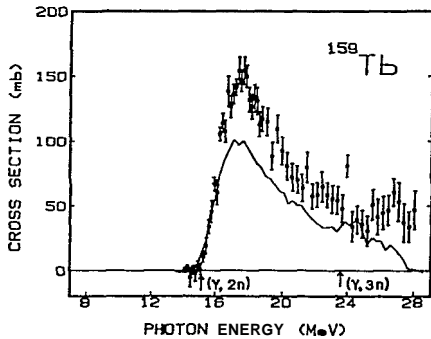
Fig.2 - $(\gamma,2n)$ cross sections from Saclay (solid line) and Livermore (experimental points) for ^{159}Tb. The Livermore data are multiplied by 1.06 in order to show both measurements at the same absolute scale.

laboratories, because these are directly measured and the partia1 cross sections are derived from the neutron multiplicity sorting.

Figure 3 shows $\sigma_{\gamma,Tn}$ from Saclay divided by $\sigma_{\gamma,Tn}$ from Livermore for ^{159}Tb. The ratio is reasonably constant and the least squares fit of a constant yields the value R = 1.062 ± 0.011. In order to compute R we interpolated $\sigma^{S}_{\gamma,Tn}$ and $o^{L}_{\gamma,Tn}$, since their data were not obtained at the same photon energies. One important conclusion can be derived from figure 3: both laboratories are detecting the same number of neutrons for all photon energies. If there were fast neutrons escaping detection in the Livermore measurements above 20 MeV, R should increase above this energy. The value of the constant R is, actually, the difference in the absolute scale of both measurements. Figure 4 shows $o^{L}_{\gamma,Tn}$ multiplied by 1.06 and $o^{S}_{\gamma,Tn}$, just to illustrate the good agreement between them, when they are plotted on the same absolute scale.

Since both laboratories agree as to the total number of neutrons detected, the differences in their (γ,n) and $(\gamma,2n)$ cross sections arise from the separation of the total counts into (γ,n) and $(\gamma,2n)$ events (neutron multiplicity sorting procedure).

If we assume that the excess (γ,n) cross section in the Saclay measurement is due to $(\gamma,2n)$ events interpreted as two (γ,n) events, that is, if we compute

$$o^{S}_{\gamma,2n} = \sigma^{S}_{\gamma,2n} + \frac{1}{2}(\sigma^{S}_{\gamma,n} - 1.06\, o^{L}_{\gamma,n}) \tag{2}$$

we obtain for $\sigma^{S}_{\gamma,2n}$ the solid line shown in figure 5. The modified $o_{\gamma,2n}$
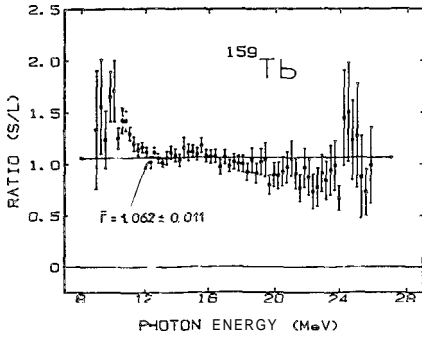
61

Fig.3 - $\sigma_{\gamma,Tn}$ from Saclay divided by $\sigma_{\gamma,Tn}$ from Livermore. $a_{\gamma,Tn}$ = $a_{\gamma,n} + 2\sigma_{\gamma,2n} + 3\sigma_{\gamma,3n}$.
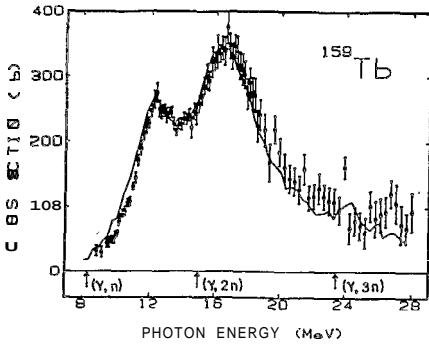

Fig.4 - $\sigma_{\gamma,Tn}$ from Livermore multiplied by 1.06 (experimental points) and $\sigma_{\gamma,Tn}$ from Saclay (solid line). $\sigma_{\gamma,Tn} = \sigma_{\gamma,n} + 2\sigma_{\gamma,2n} + 3\sigma_{\gamma,3n}$.
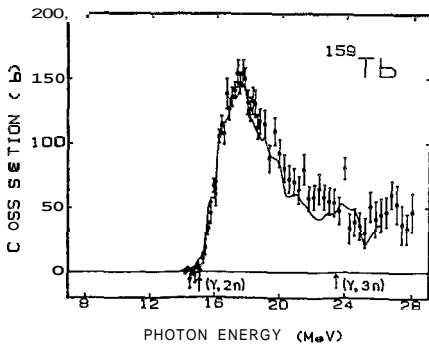

Fig.5 - $\sigma_{\gamma,2n}$ from Livermore (experimental points) and the modified (see text) $\sigma_{\gamma,2n}$ from Saclay (solid line).

cross section from Saclay agrees well with the $(\gamma,2n)$ cross section from Livermore multiplied by 1.06 (data points).

The same analysis carried out for [159]Tb was repeated for the nuclei listed in table 1. The results obtained for $\sigma_{\gamma,Tn}$ are shown in part a) of figures 6 to 17, where the solid line represents the Saclay data and the experimental points are from Livermore.

The ratio $\sigma^S_{\gamma,Tn}/\sigma^L_{\gamma,Tn}$ is shown in part b) of figures 6 to 17. The solid line in each figure results from the least squares fit of a constant to the ratio. For [118]Sn, [120]Sn, [165]Ho and [181]Ta, figures 9,10, 14 and 15, the fitting of a constant is not statistically acceptable, but a comparison between $\sigma_{\gamma,Tn}$ from Livermore and Saclay indicates a displacement in the energy scale, because the peaks do not coincide in energy (see as an example figure 14-a) for [165]Ho). The ratio $\sigma^S_{\gamma,Tn}/a^L_{\gamma,Tn}$ was also calculated with a variable energy displacement $\underline{d}$. The displacement that yields a minimum of the χ^2 for fitting a constant to the ratio was chosen. Figures 18 to 23 show the data from Saclay and Livermore, with the Livermore data displaced by $\underline{d}$. The value of $\underline{d}$ is given in part a) of the figures for each nucleus. The displacement was negative in all cases, that is, the Livermore data were shifted to lower energies. The displacement of the energy scale of the Livermore data is arbitrary and, of course, the same results can be obtained if the Saclay energy scale is moved up in energy by the same amount. For the nuclei shown in figures 18 to 23, the displacement of the energy scale improves the agreement between the shapes of $\sigma_{\gamma,Tn}$, that is, the peaks coincide in energy (compare, as an example, figures 14-a) and 21-a) for [165]Ho).

If we accept the displacement of the energy scale, we can conclude that for all nuclei analyzed here, the measurements from Saclay and Livermore are in good agreement as to the total number of emitted neutrons versus the incident photon energy, apart from an overall normalization constant. The differences between their (γ,n) and $(\gamma,2n)$ cross sections arise from differences in their neutron multiplicity sorting procedures.

In order to compare the (γ,n) and $(\gamma,2n)$ cross sections from both laboratories on the same energy scale, the Livermore data shown in all figures c), d), e) and f) are multiplied by R.

In figures 6-c) to 23-c) we show again the $\sigma_{\gamma,\text{Tn}}$ cross sections, just to illustrate the good agreement between them, when they are plotted on the same absolute scale.

In figures 6-d) to 23-d) and 6-e) to 23-e) the (γ,n) and $(\gamma,2n)$ cross sections from Livermore and Saclay are shown. Like for [159]Tb, above the $(\gamma,2n)$ threshold the (γ,n) cross sections from Saclay are always bigger than the corresponding Livermore cross sections and the $(\gamma,2n)$ cross sections from Saclay are always smaller than those from Livermore.

If the Saclay $(\gamma,2n)$ cross sections are modified using equation (2), the resulting $\sigma_{\gamma,2n}^S$ agree well with the Livermore $(\gamma,2n)$ cross sections, as shown in figures 6-f) to 23-f).

In conclusion, the differences between the shapes. and magnitudes of the Saclay and Livermore (γ,n) and $(\gamma,2n)$ cross sections are caused by the difference in the analysis that separates the total counts into (γ,n) and $(\gamma,2n)$ events.

In order to distinguish a $(\gamma,2n)$ event from two (γ,n) events, highly efficient 4π neutron detectors are needed (since the efficiency for detecting two neutrons is the square of that for one). Both Saclay and Livermore use a slowing down type of detector, in which the neutrons produced during the short beam burst of a pulsed accelerator are moderated before being detected between beam bursts. Livermore uses a large array of $^{10}BF_3$ tubes, disposed in concentric rings, embedded in a paraffin ar polyethylene matrix, and Saclay uses a large liquid scintillador. In order to be able to measure absolute cross sections and to differentiate between a $(\gamma,2n)$ event and two (γ,n) events, the detector effieiency must be known rather precisely.

The Livermore group has developed the ring-ratio teehnique for measuring the average neutron energy[19], baçed on the fact that the ratio of the countfng rate in the outer ring of $^{10}BF_3$ detectors to that in the inner ring is a strong, monotonically increasing function of the energy of the photoneutrons. With the aid of calibrated neutron sources the efficiency is determined as a function of neutron energy. Thus for every data run the average neutron energies for the (y,xn) events are determined çeparately using the ring ratio measurements[19]. This enables the partial cross sections to be obtained using detector efficiencies

appropriate to each photoneutron multiplicity, improving the
accuracy of the branching ratios.

The large Gd-loaded liquid scintillator used by Saclay was
calibrated only by means of a ^{252}Cf source. A calculated efficiency is
used to justify a constant value for the efficiency used in the photo-
neutron multiplicity sorting, on the basis that serious discrepancies
arise only above neutron energies $E_n \cong 5$ MeV, whereas the energy of most
photoneutrons does not exceed - 3 MeV[20]. Furthermore, even though the
efficiency ε measured with the ^{252}Cf source is very close to one, the
system is usually operated under timing conditions that reduce E to 0.6 [3].

The overall detector efficiencies over the range of neutron
energies relevant for giant resonance measurements are rather well known
(to < 3%)[20], so that the differences in the absolute scales of both Lab-
oratorles are primarily caused by uncertainty in the photon flux measu-
rements. However, the branching between the various partial cross sec-
tions depends critically upon the efficiencies used, since for the
(γ,xn) cross section the efficiency enters as ε^x. Thus, the fact that
both laboratories agree, for all measured nuclei, as to the total number
of emitted neutrons, apart from a constant factor due to differences in
their absolute scales, but obtain different partial cross sections, could
be explained by an error in the efficiency used by one of them.

It is important to know which set of data has the correct neu-
tron multiplicity sorting. If Saclay has the correct partial cross sec-
tions this implies that there are large percentages of neutrons from di-
rect reactions. Table 2 shows the percentage of direct neutrons ob-
tained at Saclay from their data. However; if the Livermore data are
correct the decay of the Giant Dipole Resonance in medium and heavy nu-
clei is statistical.

3. MEASUREMENT OF (e,n) AND (e,Tn) CROSS SECTIONS

The analysis of the available photoneutron data is insufficient
to assess which laboratory is performing the multiplicity sorting cor-
rectly. In order to address this question we have measured the electro-
disintegration of ^{181}Ta by neutron emission.

The (e,Tn) cross section ($\sigma_{e,Tn} = \sigma_{e,n} + 2\sigma_{e,2n}$) of ^{181}Ta was
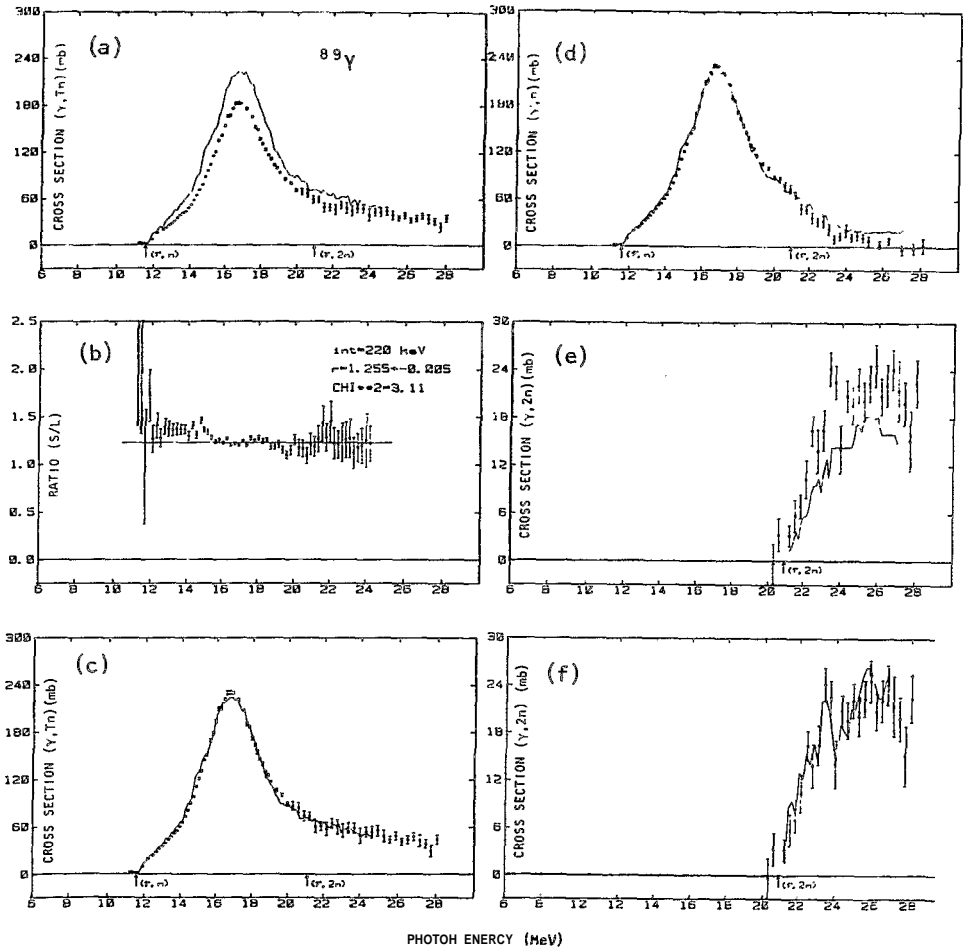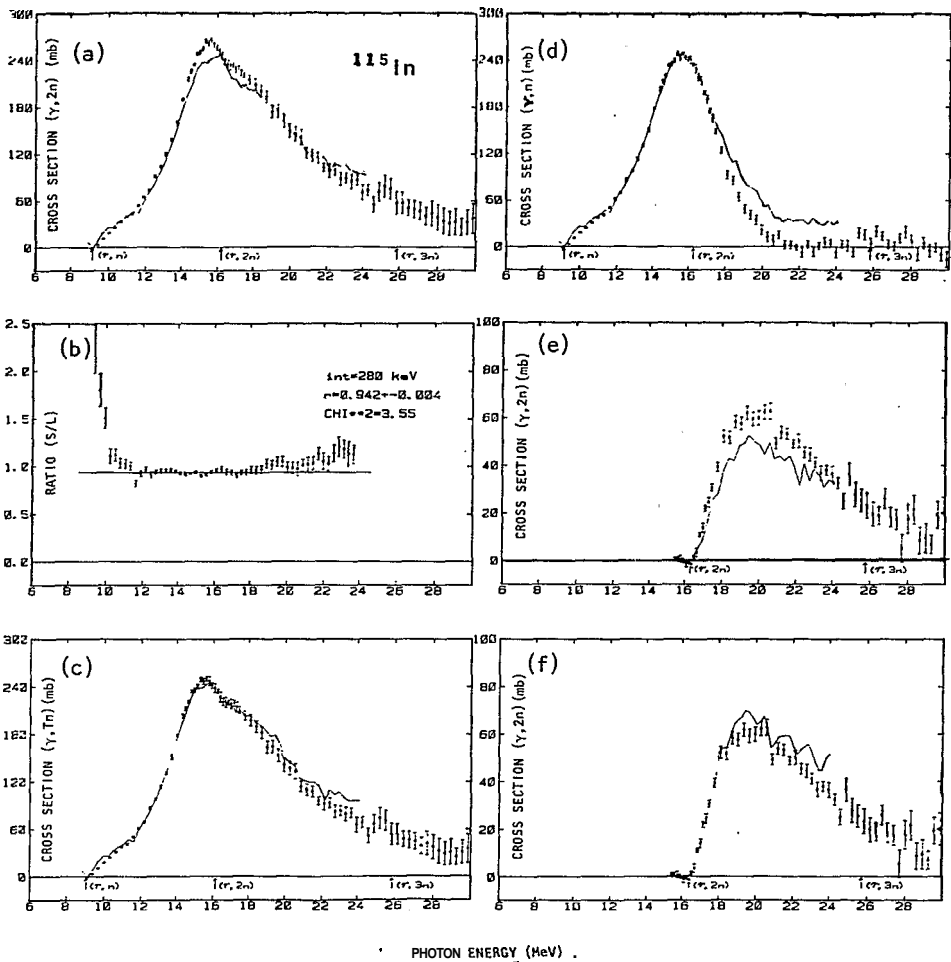
PHOTOH ENERCY (MeV)

Fig. 6 - The solid line represents the Saclay data and the experimental points are from Livermore. a) $\sigma_{\gamma,Tn} = \sigma_{\gamma,n} + 2\sigma_{\gamma,2n} + 3\sigma_{\gamma,3n}$ from Saclay and Livermore. b) $\sigma_{\gamma,Tn}$ from Saclay divided by $\sigma_{\gamma,Tn}$ from Livermore. The solid line shows R, the value obtained by fitting a constant to the ratio. c) $\sigma_{\gamma,Tn}$ from Livermore multiplied by R and $\sigma_{\gamma,Tn}$ from Saclay. d) $\sigma_{\gamma,n}$ from Livermore multiplied by R and $\sigma_{\gamma,n}$ from Saclay. e) $\sigma_{\gamma,2n}$ from Livermore multiplied by R and $\sigma_{\gamma,2n}$ from Saclay. f) $\sigma_{\gamma,2n}$ from Livermore multiplied by R and the modified $\sigma_{\gamma,2n}$ from Saclay.

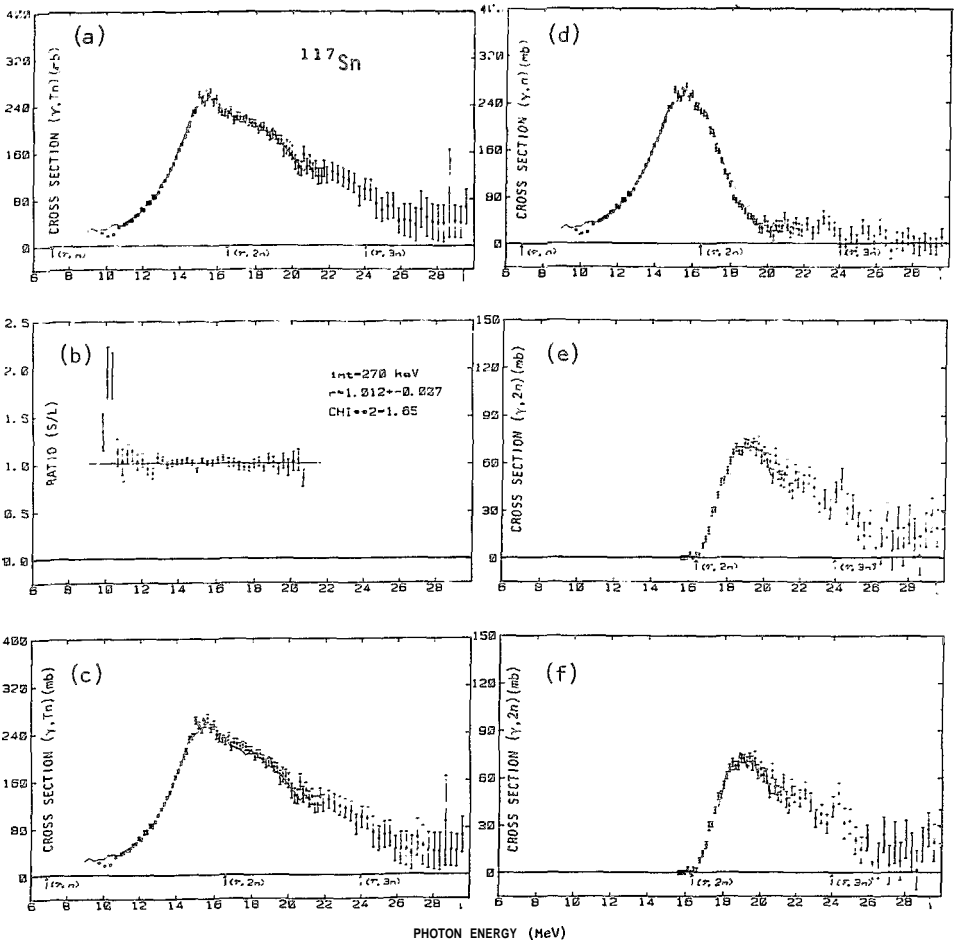$$\sigma_{\gamma,2n}^{S*} = \sigma_{\gamma,2n}^{S} + \frac{1}{2}(\sigma_{\gamma,n}^{S} - R\sigma_{\gamma,n}^{L}) \ .$$

Fig. 7 - The solid line represents the Saclay data and the experimental points are from Livermore. a) $\sigma_{\gamma,Tn} = \sigma_{y,n} + 2\sigma_{\gamma,2n} + 3\sigma_{\gamma,3n}$ from Saclay and Livermore. b) $\sigma_{\gamma,Tn}$ from Saclay divided by $\sigma_{\gamma,Tn}$ from Livermore. The solid line shows R, the value obtained by fitting a constant to the ratio. c) $\sigma_{\gamma,Tn}$ from Livermore multiplied by R and $\sigma_{\gamma,Tn}$ from Saclay. d) $\sigma_{\gamma,n}$ from Livermore multiplied by R and $\sigma_{\gamma,n}$ from Saclay. e) $\sigma_{\gamma,2n}$ from Livermore multiplied by R and $\sigma_{\gamma,2n}$ from Saclay. f) $\sigma_{\gamma,2n}$ from Livermore multiplied by R and the modified $\sigma_{\gamma,2n}$ from Saclay.

$$\sigma_{\gamma,2n}^{S*} = \sigma_{\gamma,2n}^{S} + \frac{1}{2}\left(\sigma_{\gamma,n}^{S} - R\sigma_{\gamma,n}^{L}\right).$$

67

PHOTON ENERGY (MeV)

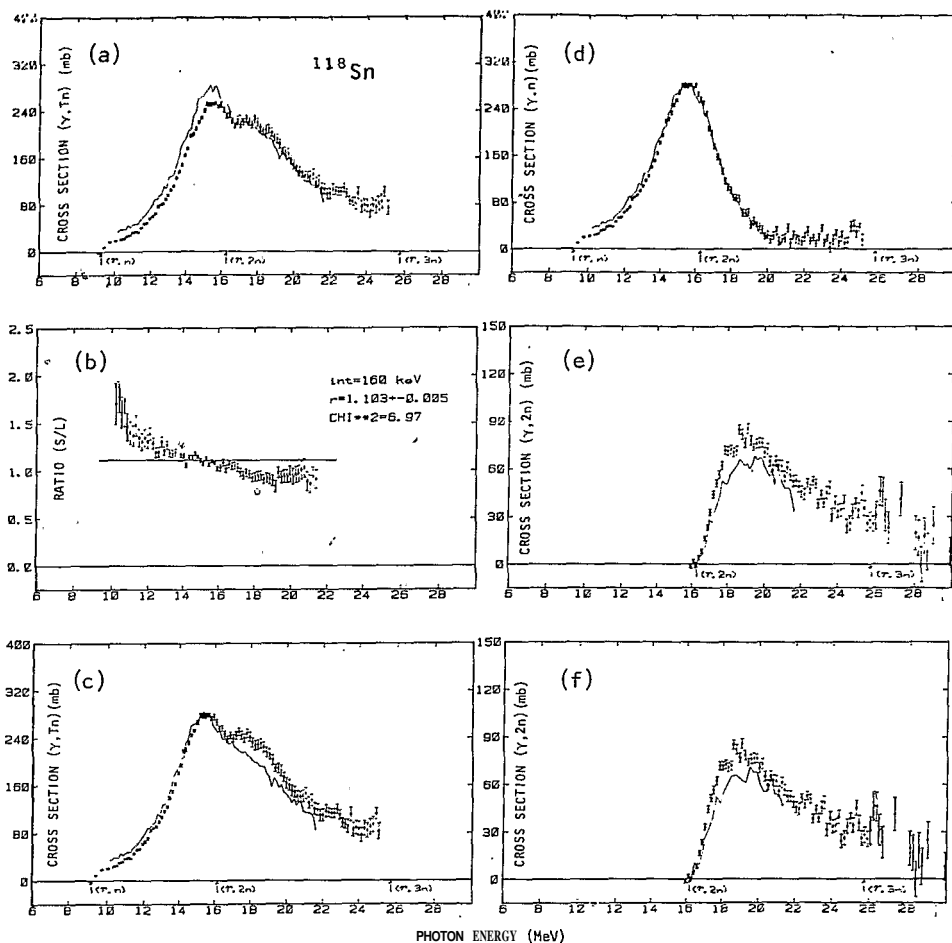Fig. 8 - The solid line represents the Saclay data and the experimental points are from Livermore. a) $\sigma_{\gamma,Tn} = \sigma_{\gamma,n} + 2\sigma_{\gamma,2n} + 3\sigma_{\gamma,3n}$ from Saclay and Livermore. b) $\sigma_{\gamma,Tn}$ from Saclay divided by $\sigma_{\gamma,Tn}$ from Livermore. The solid line shows R, the value obtained by fitting a constant to the ratio. c) $\sigma_{\gamma,Tn}$ from Livermore multiplied by R and $\sigma_{\gamma,Tn}$ from Saclay. d) $\sigma_{\gamma,n}$ from Livermore multiplied by R and $\sigma_{\gamma,n}$ from Saclay. e) $\sigma_{\gamma,2n}$ from Livermore multiplied by R and $\sigma_{\gamma,2n}$ from Saclay. f) $\sigma_{\gamma,2n}$ from Livermore multiplied by R and the modified $\sigma_{\gamma,2n}$ from Saclay.

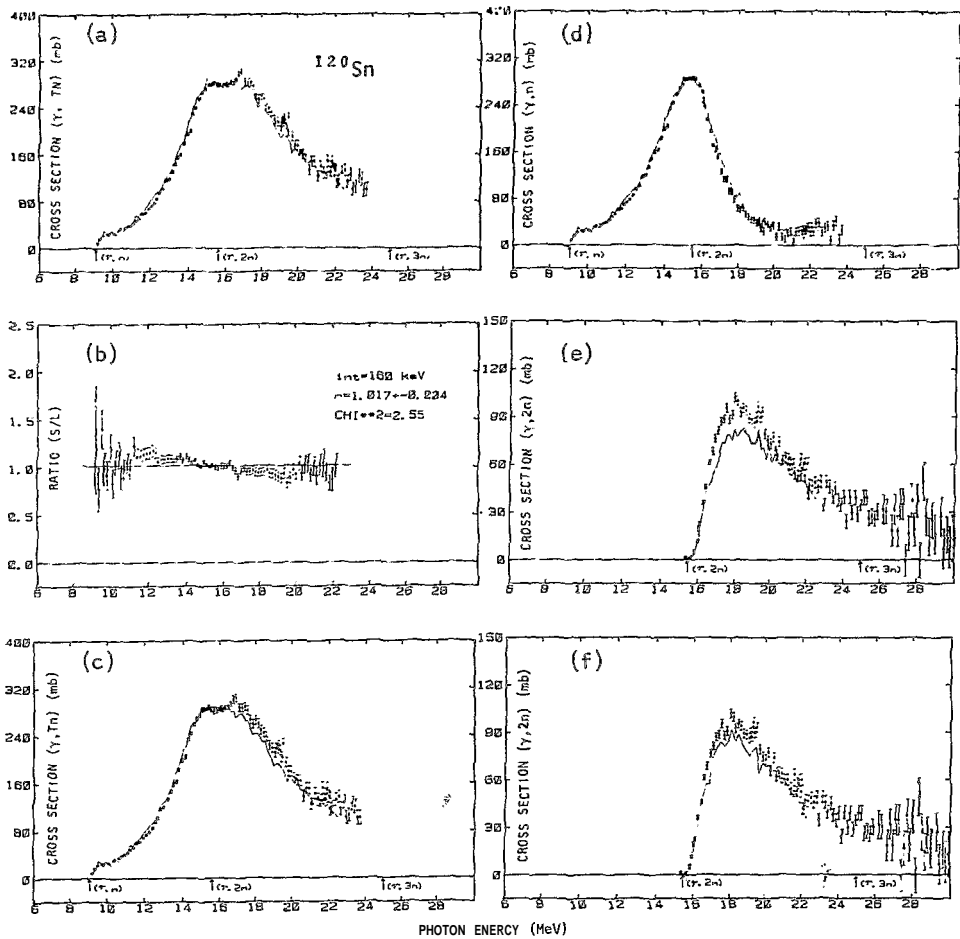$$\sigma_{\gamma,2n}^{S*} = \sigma_{\gamma,2n}^{S} + \frac{1}{2}(\sigma_{\gamma,n}^{S} - R\sigma_{\gamma,n}^{L}) \ .$$

Fig. 9 — The solid line represents the Saclay data and the experimental points are from Livermore. a) $\sigma_{\gamma,Tn} = \sigma_{\gamma,n} + 2\sigma_{\gamma,2n} + 3\sigma_{\gamma,3n}$ from Saclay and Livermore. b) $\sigma_{\gamma,Tn}$ from Saclay divided by $\sigma_{\gamma,Tn}$ from Livermore. The solid line shows R, the value obtained by fitting a constant to the ratio. c) $\sigma_{\gamma,Tn}$ from Livermore multiplied by R and $\sigma_{\gamma,Tn}$ from Saclay. d) $\sigma_{\gamma,n}$ from Livermore multiplied by R and $\sigma_{\gamma,n}$ from Saclay. e) $\sigma_{\gamma,2n}$ from Livermore multiplied by R and $\sigma_{\gamma,2n}$ from Saclay. f) $\sigma_{\gamma,2n}$ from Livermore multiplied by R and the modified $a_{\gamma,2n}$ from Saclay.

$$\sigma_{\gamma,2n}^{S*} = \sigma_{\gamma,2n}^{S} + \frac{1}{2}(\sigma_{\gamma,n}^{S} - R\sigma_{\gamma,n}^{L}).$$
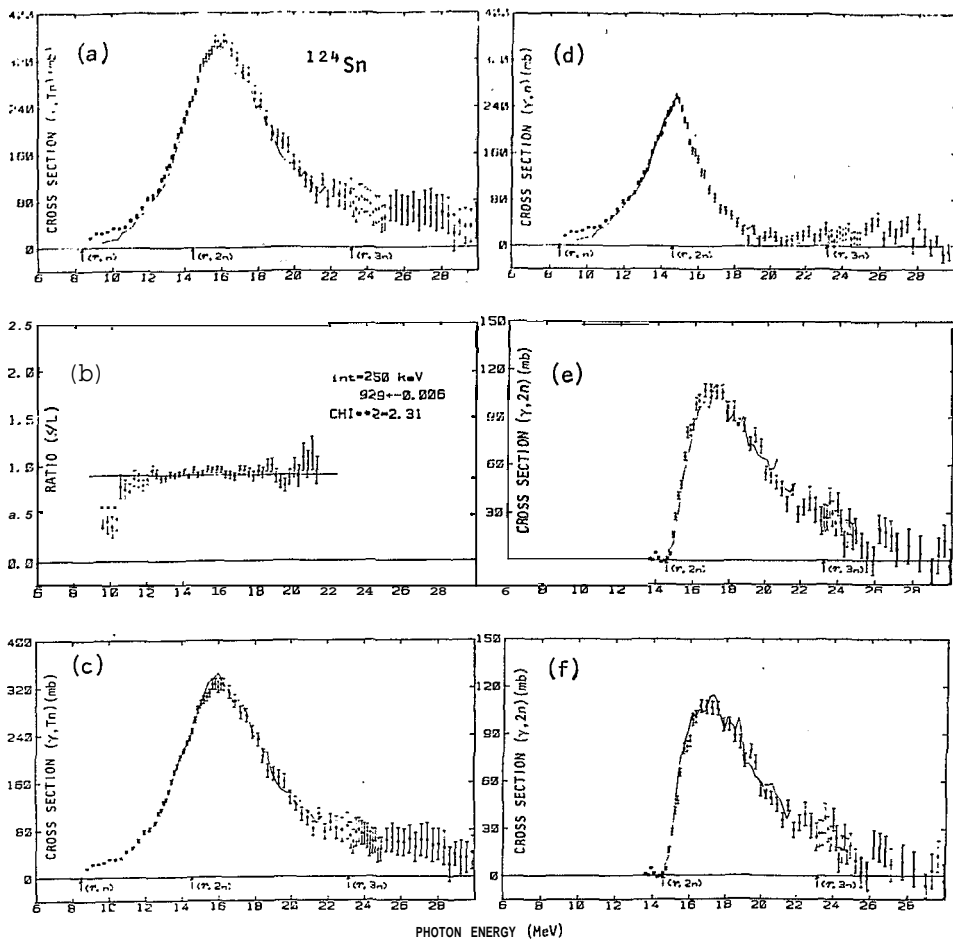
Fig. 10 - The solid line represents the Saclay data and the experimental points are from Livermore. a) $\sigma_{\gamma,Tn} = \sigma_{\gamma,n} + 2\sigma_{\gamma,2n} + 3\sigma_{\gamma,3n}$ from Saclay and Livermore. b) $\sigma_{\gamma,Tn}$ from Saclay divided by a $_{\gamma,Tn}$ from Livermore. The solid line shows R, the value obtained by fitting a constant to the ratio. c) $\sigma_{\gamma,Tn}$ from Livermore multiplied by R and $6_{\gamma,Tn}$ from Saclay. d) $\sigma_{\gamma,n}$ from Livermore multiplied by R and $\sigma_{\gamma,n}$ from Saclay. e) $\sigma_{\gamma,2n}$ from Livermore multiplied by R and $\sigma_{\gamma,2n}$ from Saclay. f) $\sigma_{\gamma,2n}$ from Livermore multiplied by R and the modified $\sigma_{\gamma,2n}$ from Saclay.

$$\sigma_{\gamma,2n}^{S*} = \sigma_{\gamma,2n}^{S} + \frac{1}{2}\left(\sigma_{\gamma,n}^{S} - R\sigma_{\gamma,n}^{L}\right) \ .$$
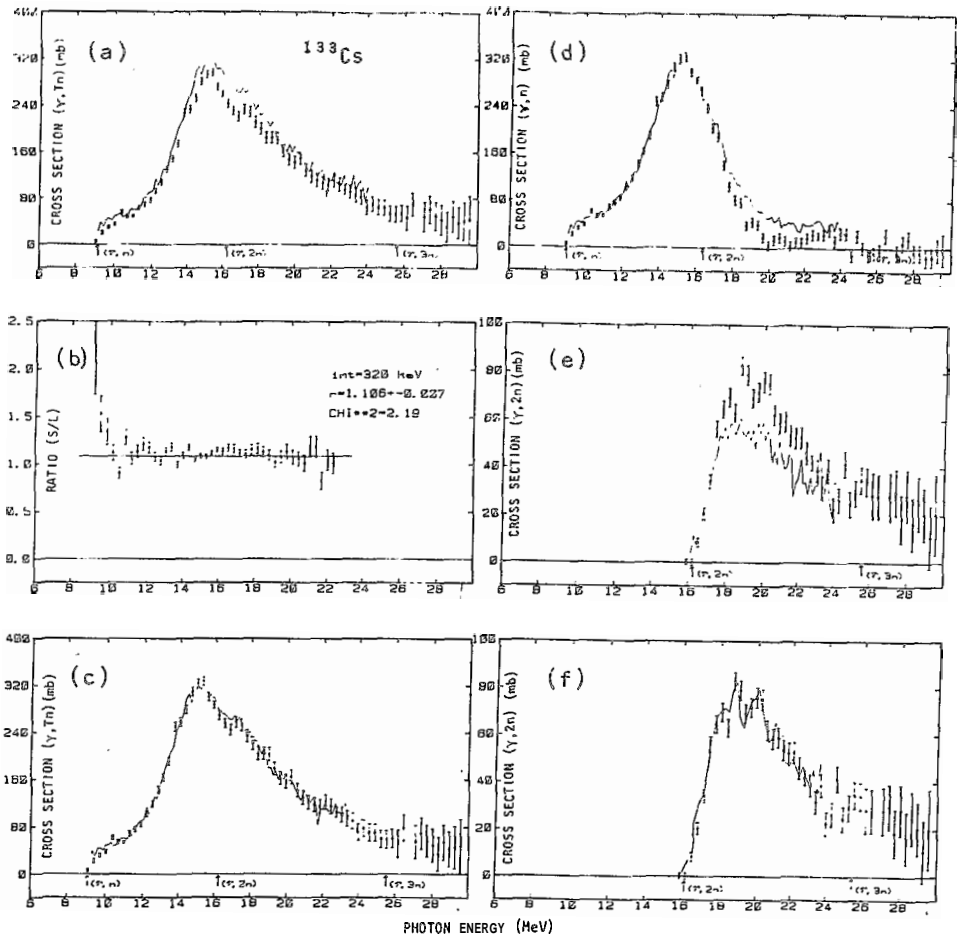
Fig. 11 - The solid line represents the Saclay data and the experimental points are from Livermore. a) $\sigma_{\gamma,Tn} = \sigma_{\gamma,n} + 2\sigma_{\gamma,2n} + 3\sigma_{\gamma,3n}$ from Saclay and Livermore. b) $\sigma_{\gamma,Tn}$ from Saclay divided by $\sigma_{\gamma,Tn}$ from Livermore. The solid line shows R, the value obtained by fitting a'constant to the ratio. c) $\sigma_{\gamma,Tn}$ from Livermore multiplied by R and $\sigma_{\gamma,Tn}$ from Saclay. d) $\sigma_{\gamma,n}$ from Livermore multiplied by R and $\sigma_{\gamma,n}$ from Saclay. e) $\sigma_{\gamma,2n}$ from Livermore multiplied by R and $\sigma_{\gamma,2n}$ from Saclay. f) $\sigma_{\gamma,2n}$ from Livermore multiplied by R and the modified $\sigma_{\gamma,2n}$ from Saclay.

$$\sigma_{\gamma,2n}^{S*} \approx \sigma_{\gamma,2n}^{S} + \frac{1}{2}(\sigma_{\gamma,n}^{S} - R\sigma_{\gamma,n}^{L}).$$
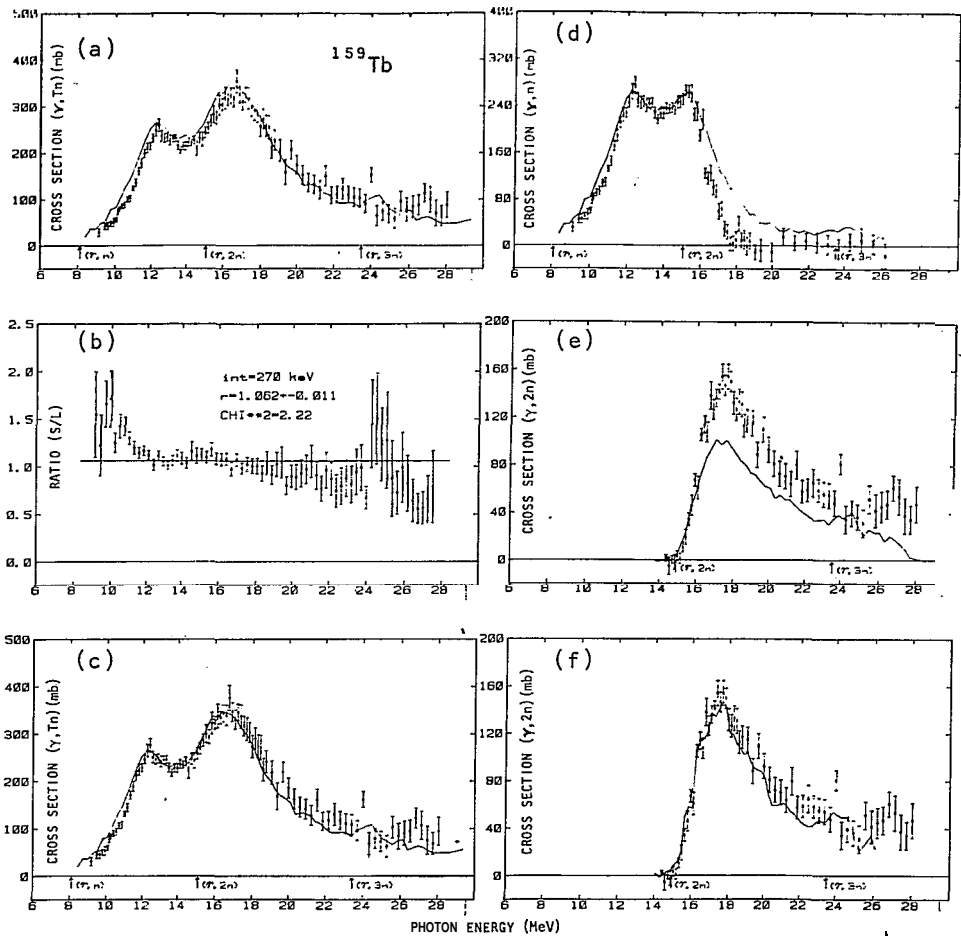
71

Fig. 12 - The solid line represents the Saclay data and the experimental points are from Livermore. a) $\sigma_{\gamma,Tn} = \sigma_{\gamma,n} + 2\sigma_{\gamma,2n} + 3\sigma_{\gamma,3n}$ from Saclay and Livermore. b) $\sigma_{\gamma,Tn}$ from Saclay divided by $\sigma_{\gamma,Tn}$ from Livermore. The solid line shows R, the value obtained by fitting a constant to the ratio. c) $\sigma_{\gamma,Tn}$ from Livermore multiplied by R and $\sigma_{\gamma,Tn}$ from Saclay. d) $\sigma_{\gamma,n}$ from Livermore multiplied by R and $\sigma_{\gamma,n}$ from Saclay. e) $\sigma_{\gamma,2n}$ from Livermore multiplied by R and $a_{\gamma,2n}$ from Saclay. f) $a_{\gamma,2n}$ from Livermore multiplied by R and the modified $\sigma_{\gamma,2n}$ from Saclay.

$$\sigma^{S*}_{\gamma,2n} = \sigma^{S}_{\gamma,2n} + \frac{1}{2}(\sigma^{S}_{\gamma,n} - R\sigma^{L}_{\gamma,n})$$

72

Fig. 13 - The solid line represents the Saclay data and the experimental points are from Livermore. a) $\sigma_{\gamma,Tn} = \sigma_{\gamma,n} + 2\sigma_{\gamma,2n} + 3\sigma_{\gamma,3n}$ from Saclay and Livermore. b) $\sigma_{\gamma,Tn}$ from Saclay divided by $\sigma_{\gamma,Tn}$ from Livermore. The solid line shows R, the value obtained by fitting a constant to the ratio. c) $\sigma_{\gamma,Tn}$ from Livermore multiplied by R and $\sigma_{\gamma,Tn}$ from Saclay. d) $\sigma_{\gamma,n}$ from Livermore multiplied by R and a $\sigma_{\gamma,n}$ from Saclay. e) $\sigma_{\gamma,2n}$ from Livermore multiplied by R and a $\sigma_{\gamma,2n}$ from Saclay. f) $\sigma_{\gamma,2n}$ from Livermore multiplied by R and the modified $\sigma_{\gamma,2n}$ from Saclay.

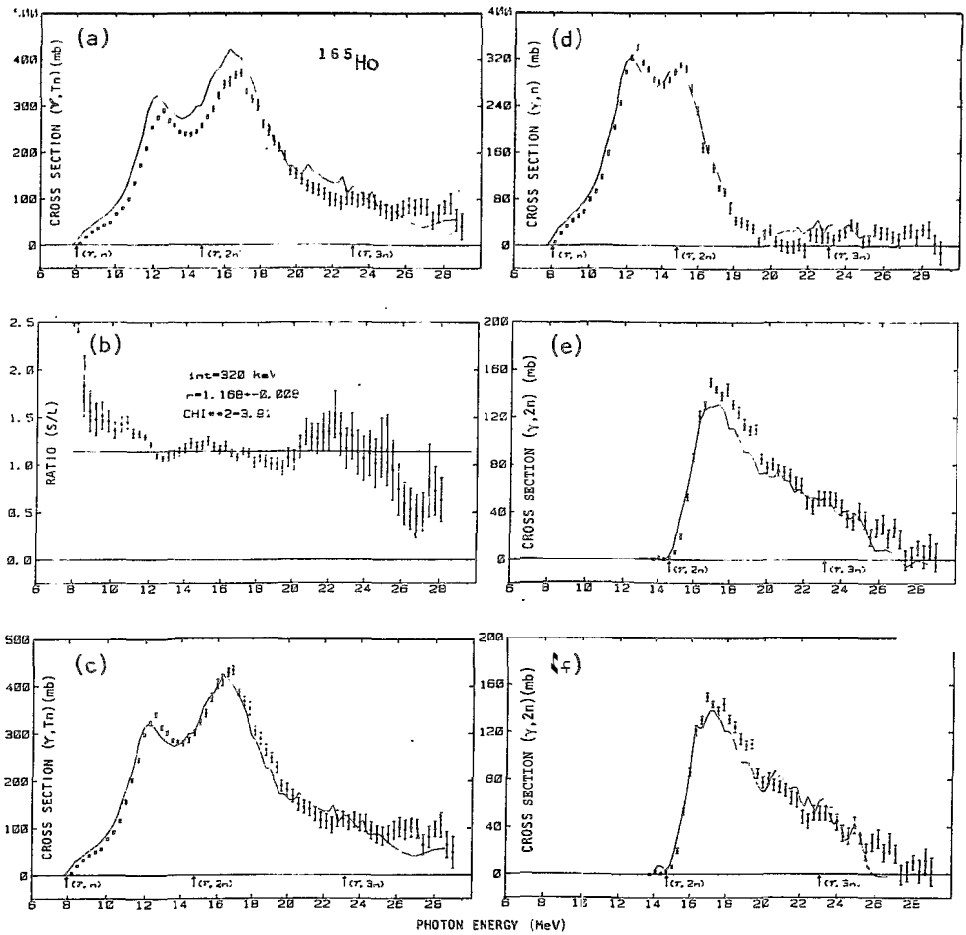$$\sigma_{\gamma,2n}^{S*} = \sigma_{\gamma,2n}^{S} + \frac{1}{2}(\sigma_{\gamma,n}^{S} - R\sigma_{\gamma,n}^{L}) .$$

Fig. 14 - The solid line represents the Saclay data and the experimental points are from Livermore. a) $\sigma_{\gamma,Tn} = \sigma_{\gamma,n} + 2\sigma_{\gamma,2n} + 3\sigma_{\gamma,3n}$ from Saclay and Livermore. b) $\sigma_{\gamma,Tn}$ from Saclay divided by $\sigma_{\gamma,Tn}$ from Livermore. The solid line shows R, the value obtained by fitting a constant to the ratio. c) $\sigma_{\gamma,Tn}$ from Livermore multiplied by R and $\sigma_{\gamma,Tn}$ from Saclay. d) $\sigma_{\gamma,n}$ from Livermore multiplied by R and $\sigma_{\gamma,n}$ from Saclay. e) $\sigma_{\gamma,2n}$ from Livermore multiplied by R and $\sigma_{\gamma,2n}$ from Saclay. f) $\sigma_{\gamma,2n}$ from Livermore multiplied by R and the modified $\sigma_{\gamma,2n}$ from Saclay.

$$\sigma_{\gamma,2n}^{S*} = \sigma_{\gamma,2n}^{S} + \frac{1}{2}(\sigma_{\gamma,n}^{S} - R\sigma_{\gamma,n}^{L}) \ .$$
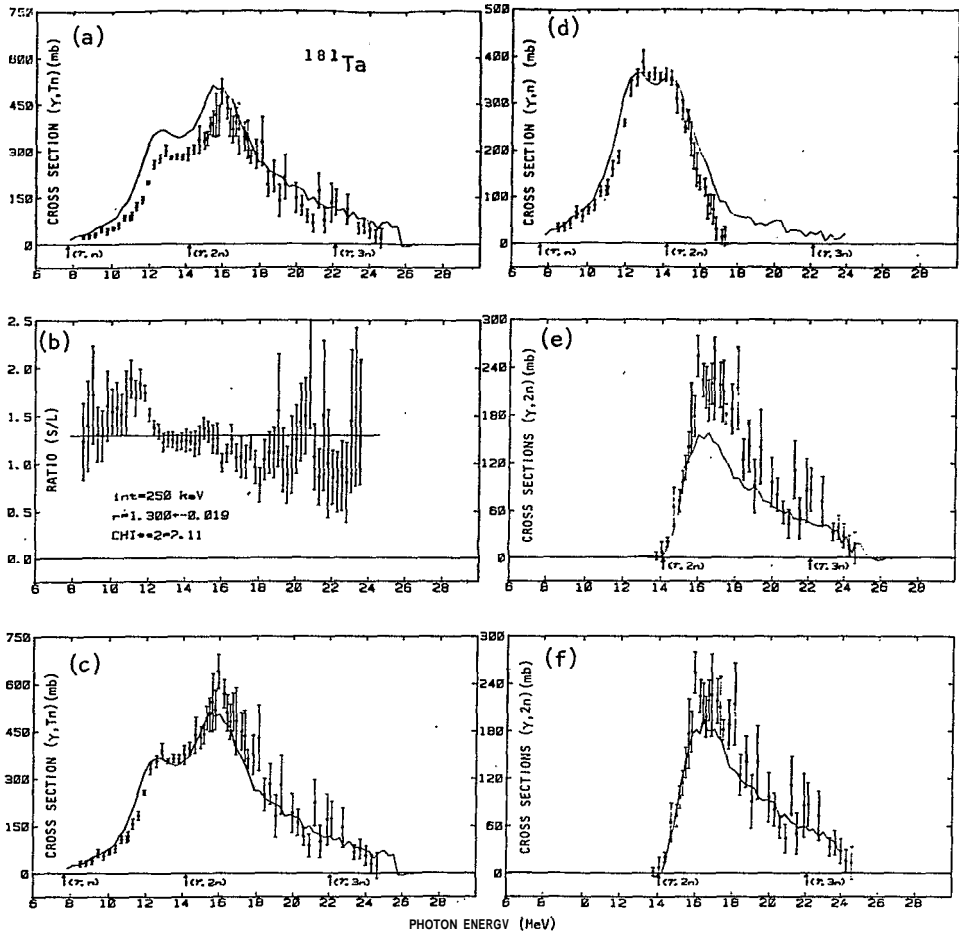
Fig. 15 - The solid line represents the Saclay data and the experimental points are from Livermore. a) $\sigma_{\gamma,Tn} = \sigma_{\gamma,n} + 2\sigma_{\gamma,2n} + 3\sigma_{\gamma,3n}$ from Saclay and Liverrnore. b) $\sigma_{\gamma,Tn}$ from Saclay divided by $\sigma_{\gamma,Tn}$ from Livermore. The solid line shows R, rhe value obtained by fitting a constant to the ratio. c) $\sigma_{\gamma,Tn}$ from Liverrnore multiplied by R and $\sigma_{\gamma,Tn}$ from Saclay. d) $\sigma_{\gamma,n}$ from Livermore multiplied by R and $\sigma_{\gamma,n}$ from Saclay. e) $\sigma_{\gamma,2n}$ from Livermore multiplied by R and $\sigma_{\gamma,2n}$ from Saclay. f) $\sigma_{\gamma,2n}$ from Livermore multiplied by R and the modified $\sigma_{\gamma,2n}$ from Saclay.

$$\sigma_{\gamma,2n}^{S*} = \sigma_{\gamma,2n}^{S} + \frac{1}{2}(\sigma_{\gamma,n}^{S} - R\sigma_{\gamma,n}^{L})$$
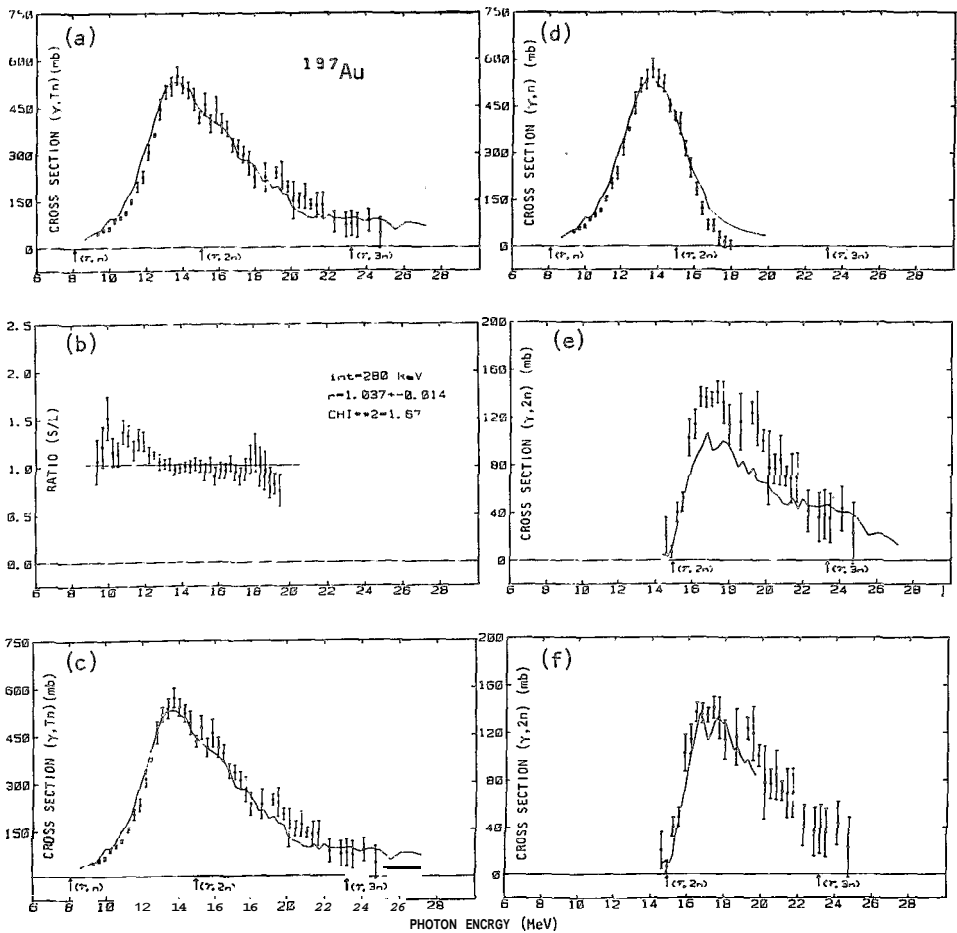
75

Fig.16 - The solid line represents the Saclay data and the experimental points are from Livermore. a) $\sigma_{\gamma,Tn} = a_{\gamma,n} + 2\sigma_{\gamma,2n} + 3\sigma_{\gamma,3n}$ from Saclay and Livermore. b) $a_{\gamma,Tn}$ from Saclay divided by $\sigma_{\gamma,Tn}$ from Livermore. The solid line shows R, the value obtained by fitting a constant to the ratio. c) $\sigma_{\gamma,Tn}$ from Livermore multiplied by R and $\sigma_{\gamma,Tn}$ from Saclay. d) $\sigma_{\gamma,n}$ from Livermore multiplied by R and $\sigma_{\gamma,n}$ from Saclay. e) $\sigma_{\gamma,2n}$ from Livermore multiplied by R and $\sigma_{\gamma,2n}$ from Saclay. f) $\sigma_{\gamma,2n}$ from Livermore multiplied by R and the modified $\sigma_{\gamma,2n}$ from Saclay.

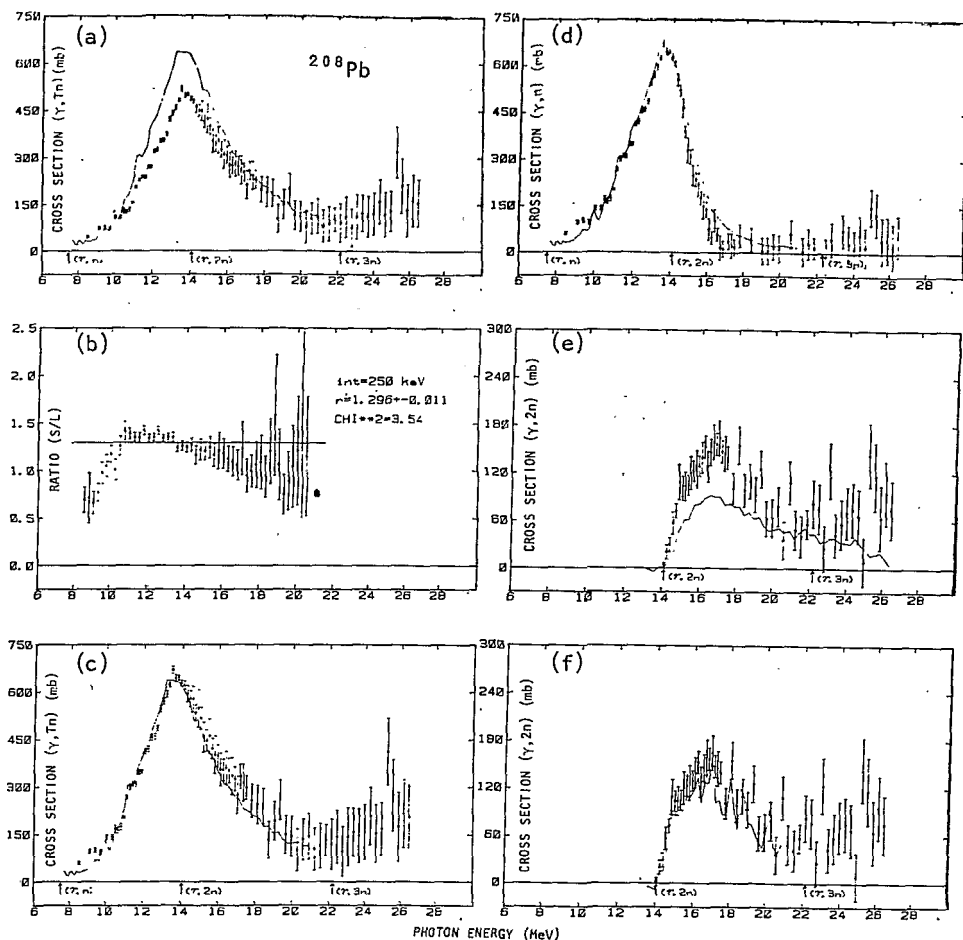$$\sigma_{\gamma,2n}^{S*} = \sigma_{\gamma,2n}^{S} + \frac{1}{2}(\sigma_{\gamma,n}^{S} - R\sigma_{\gamma,n}^{L}) \ .$$

Fig. 17 - The solid line represents the Saclay data and the experimental points are from Livermore. a) $\sigma_{\gamma,Tn} = a_{\gamma,n} + 2\sigma_{\gamma,2n} + 3\sigma_{\gamma,3n}$ from Saclay and Livermore. b) $\sigma_{\gamma,Tn}$ from Saclay divided by $\sigma_{\gamma,Tn}$ from Livermore. The solid line shows R, the value obtained by fitting a constant to the ratio. c) $\sigma_{\gamma,Tn}$ from Livermore multiplied by R and $\sigma_{\gamma,Tn}$ from Saclay. d) $\sigma_{\gamma,n}$ from Livermore multiplied by R and $\sigma_{\gamma,n}$ from Saclay. e) $\sigma_{\gamma,2n}$ from Livermore multiplied by R and $\sigma_{\gamma,2n}$ from Saclay. f) $\sigma_{\gamma,2n}$ from Livermore multiplied by R and the modified $a_{\gamma,2n}$ from Saclay.

$$\sigma_{\gamma,2n}^{S*} = \sigma_{\gamma,2n}^{S} + \frac{1}{2} (\sigma_{\gamma,n}^{S} - R\sigma_{\gamma,n}^{L}).$$
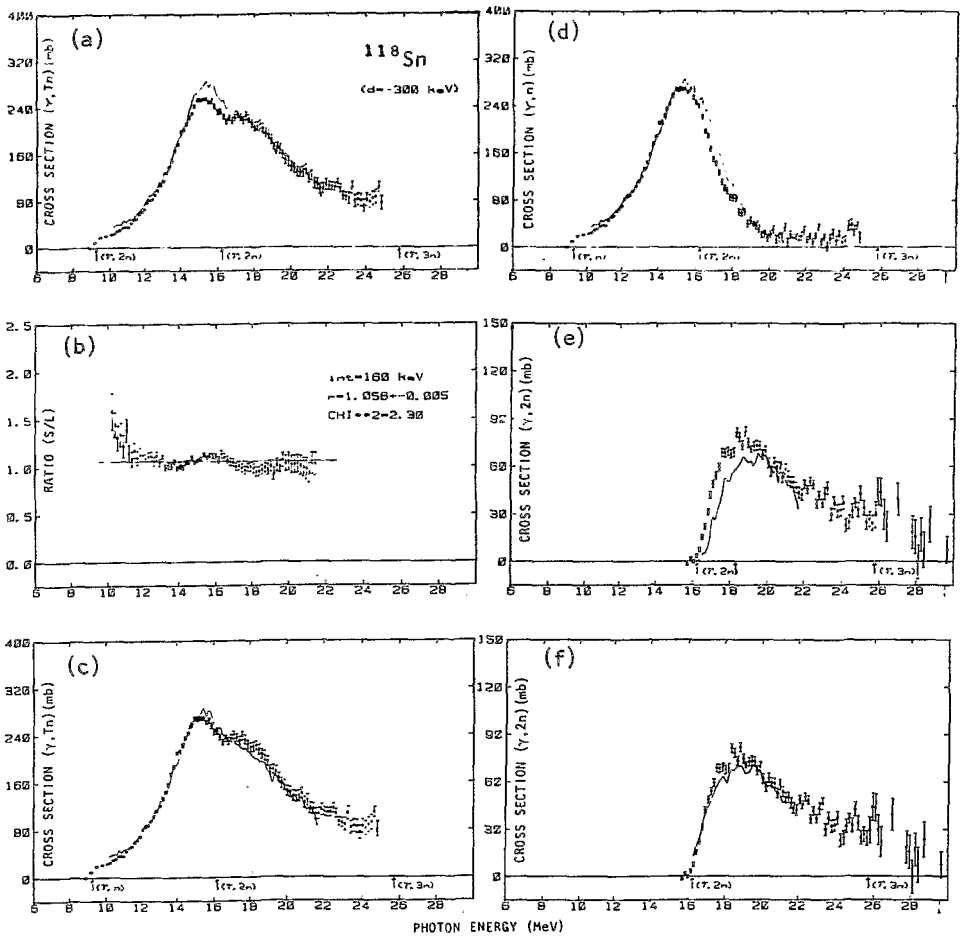
Fig. 18 - a) $\sigma_{\gamma,\text{Tn}}$ from Saclay and Livermore. The energy scale of the Livermore data is displaced by d. The value of the displacement is given in each figure. b), c), d), e) and f) - The same as for figures 1 to 12.
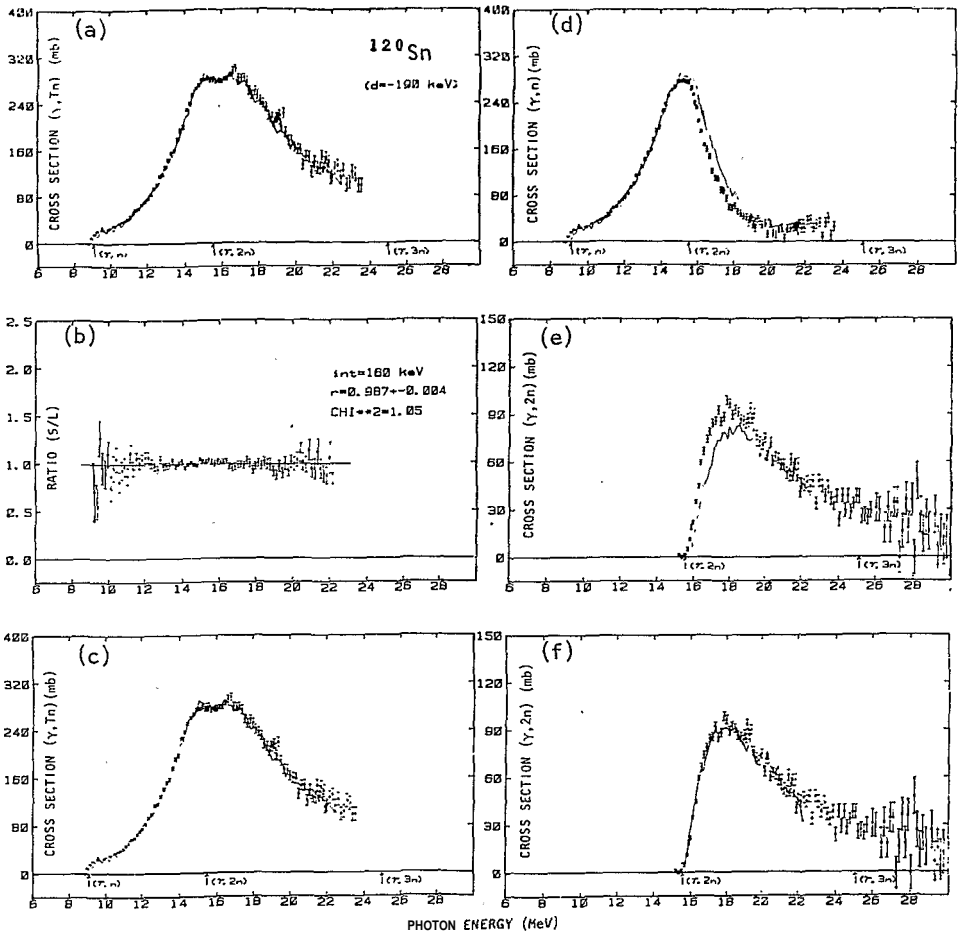
Fig. 19 - a) $\sigma_{\gamma,Tn}$ from Saclay and Livermore. The energy scale of the Livermore data is displaced by $\underline{d}$. The value of the displacement is given in each figure. b), c), d), e) and f) - The same as for figures 1 to 12.
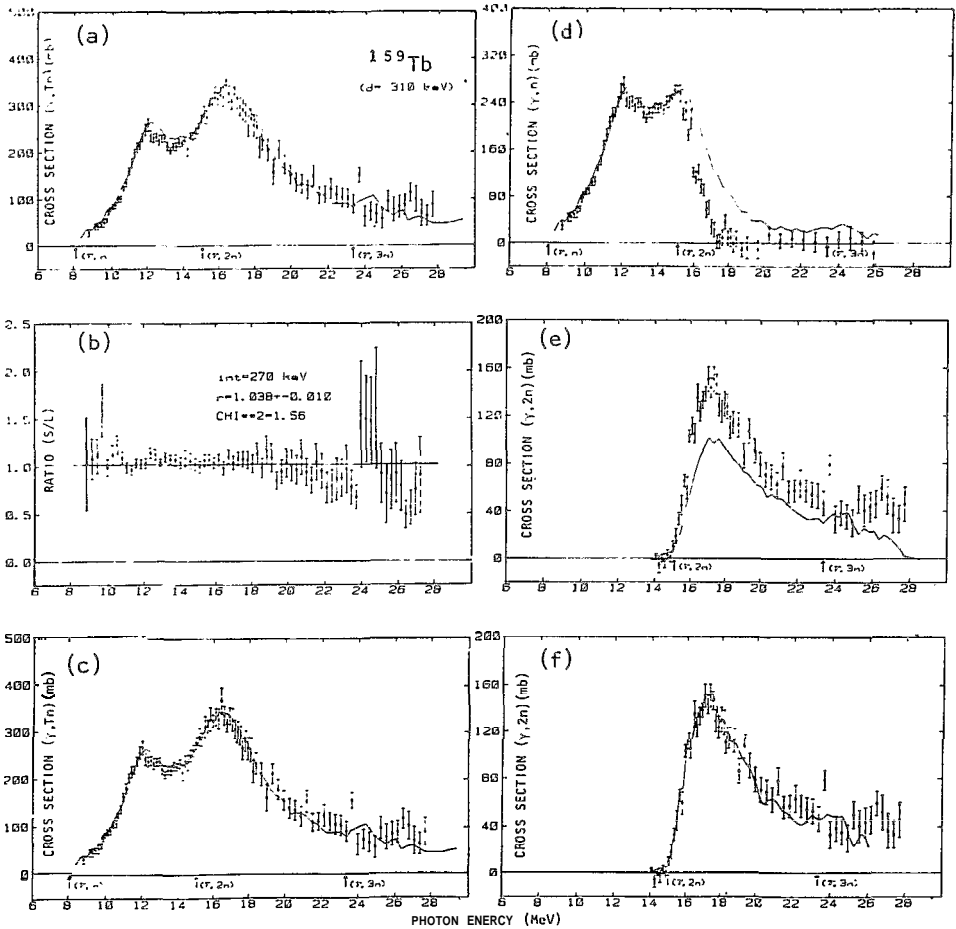
Fig. 20 - a) $a_{\gamma,Tn}$ from Saclay and Livermore. The energy scale of the Livermore data is displaced by $\underline{d}$. The value of the displacement is given in each figure. b), c), d), e) and f) - The same as for figures 1 to 12.

Fig. 21 - a) $\sigma_{\gamma,Tn}$ from Saclay and Livermore. The energy scale of the Livermore data is displaced by $\underline{d}$. The value of the displacement is given in each figure. b), c), d), e) and f) - The same as for figures 1 to 12.
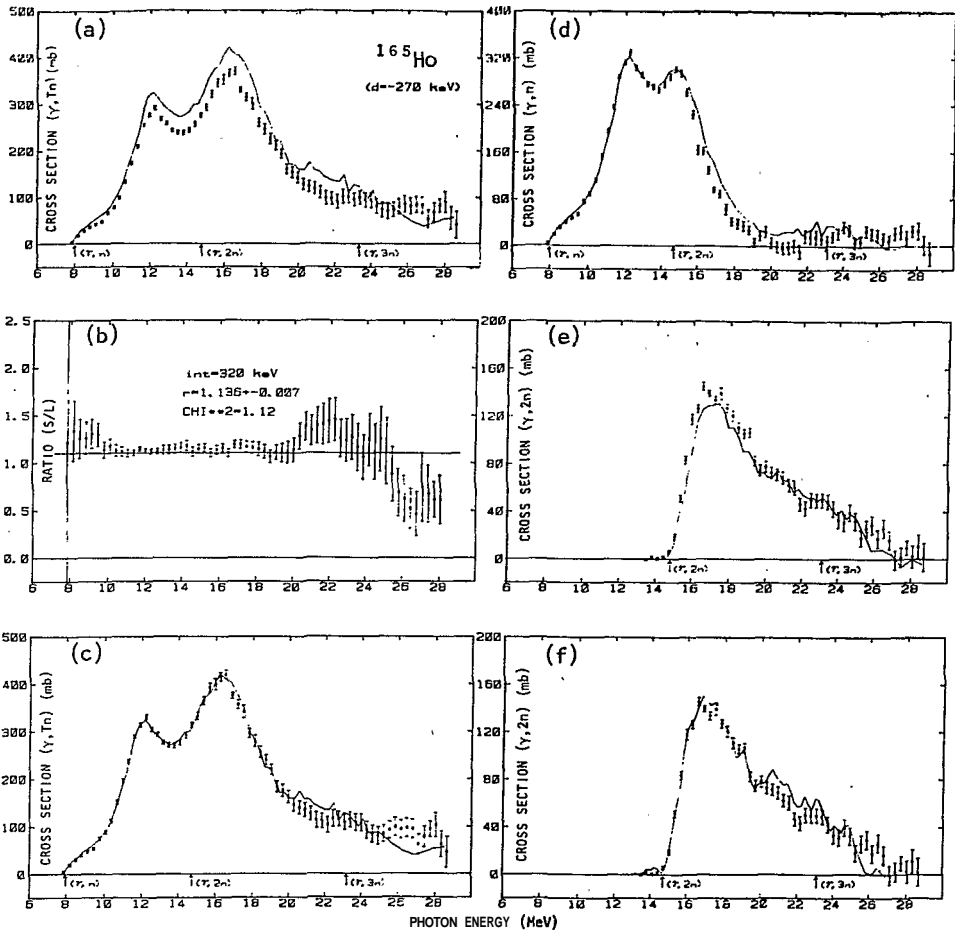
Fig. 22 - a) $\sigma_{\gamma, \text{Tn}}$ from Saclay and Livermore. The energy scale of the Livermore data is displaced by $\underline{d}$. The value of the displacement is given in each figure. b), c), d), e) and f) - The same as for figures 1 to 12.
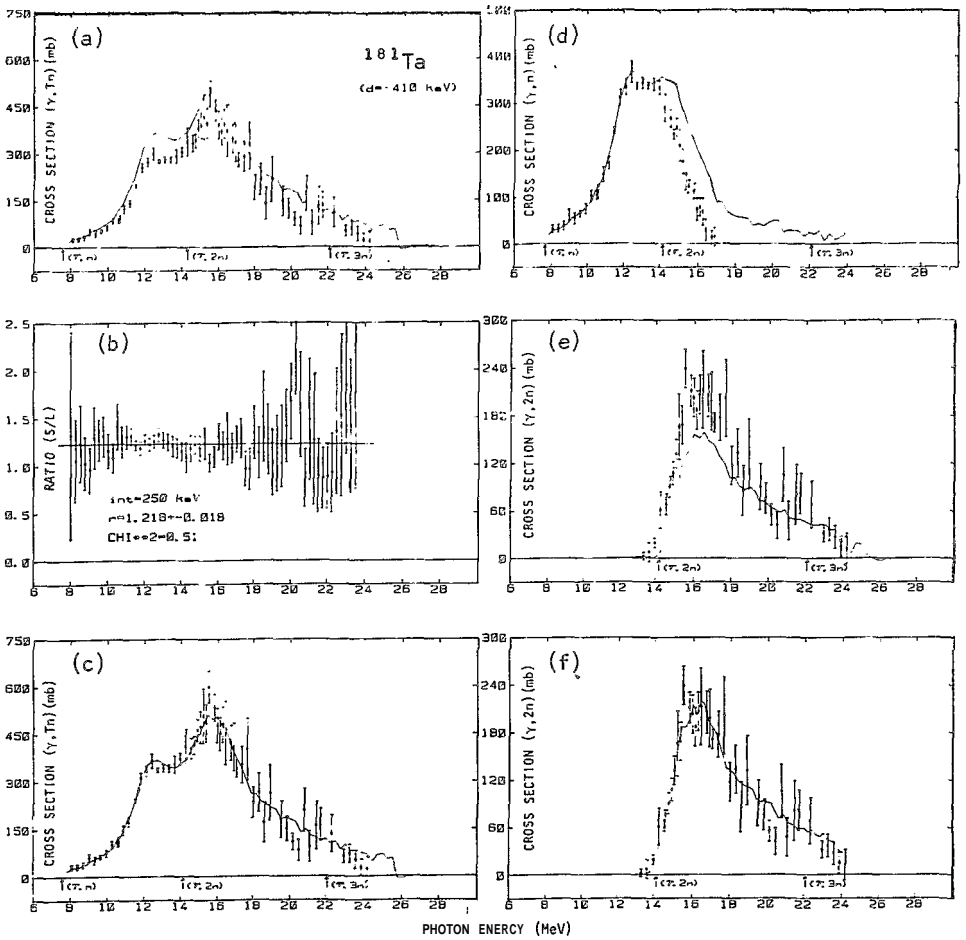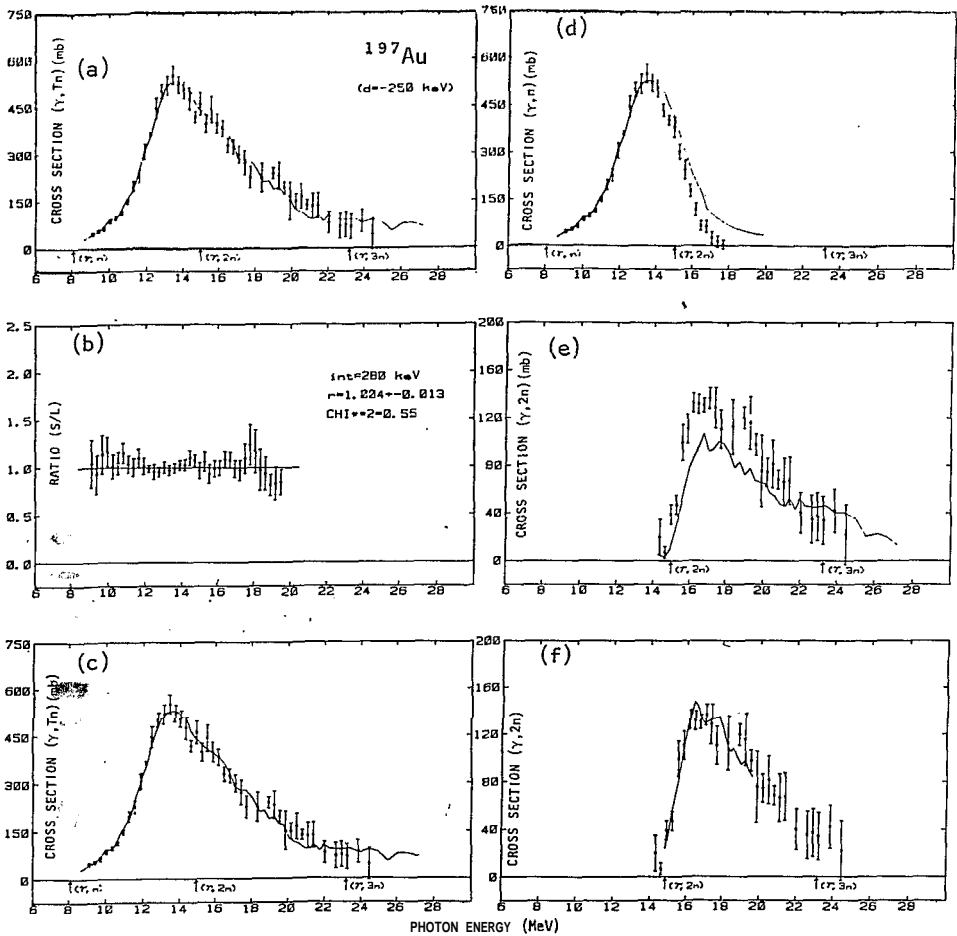
Fig. 23 - a) $\sigma_{\gamma, Tn}$ from Saclay and Livermoce. The energy scale of the Livermore data is displaced by <u>d</u>. The value of the displacement is given in each figure. b), c), d), e) and f) - The same as for figures 1 to 12.

measured by counting the emitted neutrons. The detector system consists of four $^{10}BF_3$ counters embedded in paraffin. The (e,n) cross section was measured by residual activity, following the 93.3 keV γ-ray line that results from the decay of ^{180}Ta to ^{180}Hf, using a Ge(Li) detector. The results obtained for the (e,n) cross section are shown in fig. 24 by the triangles. The agreement between the (e,n) cross section measured by radioactivity and by counting the neutrons (up to the (γ,2n) threshold) is very good, the ratio of the two cross sections being a constant as a function of electron energy. The weighted average of the neutron detection/residual activity ratio is 1.057 ± 0.023 and the results sbtained for (e,Tn) (shown in fig. 24 by the open circles) have been divided by this factor in order to make them compatible with $\sigma_{e,n}$.

The ^{181}Ta(e,2n) cross section can be easily derived from the data of fig. 24

$$\sigma_{e,2n}(E_0) = |\sigma_{e,Tn}(E_0) - \sigma_{e,n}(E_0)|/2$$

and is shown in this same figure by the full circles. Further details of this experiment are given in ref. 21.

Electro aiid photodisintegration cross sections are related by the virtual photon spectra[22,23], making it possible to predict the ^{181}Ta(e,2n) cross section from the existing data of (γ,2n) from bsth Saclay and Livermore laboratories. The predicted cross section are shown respectively by the solid lines S and L in fig. 24. Our results are in good agreement with the (e,2n) cross section calculated using the Livermore (γ,2n) data and excludes the result obtained using the Saclay cross section. The inclusion in the (γ,2n) cross section of an E2 strength ammounting to one isovector E2 sum makes little difference in the predicted cross sections, as can be seen by the dashed lines infig. 24. This indicates that Livermore is correctly performing the neutron multiplicity sorting.

4. CONCLUSIONS

The differences between the Saclay and Livermore photoneutron cross sections arise from the analysis that separates the total counts
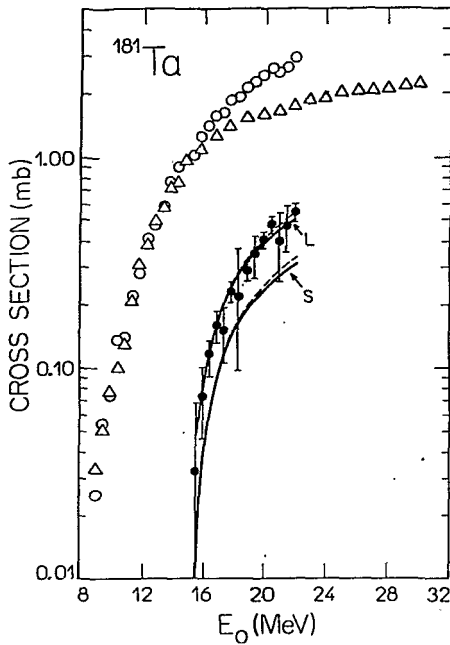
Fig. 24 - Measured $\sigma_{e,Tn}$ (circles) and $\sigma_{e,n}$ (triangles) and obtained $\sigma_{e,2n}$ (full circles) versus electron incident energy. The solid lines show the predicted $\sigma_{e,2n}$ cross sections using Saclay and Livermore data for $\sigma_{\gamma,2n}$.

in partial cross sections (neutron multiplicity sorting).

Our determination of the (e,2n) cross section in ^{181}Ta shows that the neutron multiplicity sorting from Livermore is correct. There are two important consequences from that:

a) There are no large percentages of direct neutrons emitted from the El Giant Resonance. The decay of the El Giant Resonance is dominantly statistical.

b) The error in the Saclay neutron multiplicity sorting could seriously affect their more recent results for total photoabsorption.

Further measurements are needed to establish the corre'ct shapes and magnitudes of photoneutron cross sections as well measurements of total photoabsorption in heavy nuclei where large neutron multiplicities are involved.

REFERENCES

1. Atlas of photoneutson cross sections obtained with monoenergetic photons, Bicentennial Edition, Preprint UCRL-78482, edited by B.L. Berman and B.L.Berman, Rev.Mod.Phys. 47, 713 (1975).

2. R.Bergere, Lecture Notes in Physics 61, 1 (1977) and G.Ricco, Lecture Notes in Physics 61, 223 (1977).

3. A.Lepretre, H.Beil, R.Bergere, P.Carlos, A. Veyssiere and M.Sugawara, Nucl. Phys. A175, 609 (1971).

4. B.L.Berman, J.T.Caldwell, R.R.Harvey, M.A.Kelly, R.L.Bramblett and S.C.Fultz, Phys. Rev. A175, 1098 (1967).

5. A.Lepretre, H.Beil, R.Bergere, P.Carlos, A.Deminiac and A.Veyssiere, Nucl. Phys. A219, 39 (1974).

6. S.C.Fultz, B.L.Berman, J.T.Caldwell, R.L.Bramblett and M.A. Kelly, Phys. Rev. 186, 1255 (1969).

7. B.L.Berman, R.L.Bramblett, J.T.Caldwell, H.S.Davis, M.A. Kelly and S.C.Fultz, Phys. Rev. 177, 1745 (1969).

8. R.L.Bergere, H.Beil and A.Veyssiere, Nucl. Phys. A121, 463 (1968).

9. R.L.Bramblett, J.T.Caldwell, R.R.Harvey and S.C.Fultz, Phys. Rev. B133, 869 (1964).

10. B.L.Berman, M.A.Kelly, R.L.Bramblett, J.T.Caldwell, H.S.Davis and S.C.Fultz, Phys. Rev. 185, 1576 (1969).

11. R.L.Bramblett, J.T.Caldwell, G. F.Auchampaugh and S.C.Fultz, Phys, Rev. 129, 2723 (1963).

12. A.Veyssiere, H.Beil, R.Bergere, P.Carlos and A. Leprete, Nucl.Phys. A159, 561 (1970).

13. S.C.Fultz, R.L.Bramblett, J.T.Caldwell and N.A.Kerr, Phys. Rev.127, 1237 (1962).

14. R.R.Harvey, J.T.Caldwell, R.L.Bramblett and S.C.Fultz, Phys. Rev. B136, 126 (1964).

15. E.Wolynec, A.R.V.Martinez, P.Gouffon, Y.Miyao, V.A.Serrão and M.N. Martins, Phys. Rev. C29, 1137 (1984).

16. H. Beil, R.Bergere, P.Carlos, A.Lepretre, A.Deminiac and A.Veyssiere, Nucl. Phys. A227, 427 (1974). .

17. R.Bergere, H.Beil, P.Carlos and A.Veyssiere, Nucl. Phys. A133, 417 (1969).

18. A.Veyssiere, H.Beil, R.Bergere, P.Carlos, A.Lepretre and K.Kernbach, Nucl.Phys. A*199*, 45 (1973).

19. B.L.Berman and S.C.Fultz, Rev. Mod. Phys. 47, 713 (1975).

20. H.Beil, R.Bergere and A.Veyssiere, Nucl. Instr. and Meth. 67, 293 (1969).

21. E.Wolynec, V.A.Serrão, P.Gouffon, Y.Miyao and M.N.Martins, Submitted to J. Phys. G.

22. W.W.Gargaro and D.S.Onley, Phys. Rev. C*4*, 1032 (1971) and C.W. Soto' Vargas, D.S.Onley and L.E. Wright, Nucl. Phys. A*288*, 45 (1977).

23. W.R.Dodge, E.Hayward and E.Wolynec, Phys. Rev. C28, 150 (1983).

Resumo

Este trabalho discute as diferenças existentes entre as seções de choque de fotonêutrons medidas nos Laboratórios de Saclay e Livermore Mostramos que as discrepâncias entre as seções de choque (γ,n) e $(\gamma,2n)$ obtidas por esses Laboratórios se originam no processo de separação de multiplicidades dos nêutrons. Medidas das seções de choque (e,n) e $(\gamma,2n)$ no ^{181}Ta mostram que o Laboratório de Livermore faz a separação de multiplicidades correta. As implicações desses resultados são discutidas.